

See discussions, stats, and author profiles for this publication at: <https://www.researchgate.net/publication/301620370>

# Nummulite biostratigraphy of the Eocene succession in the Bahariya Depression, Egypt: Implications for timing of iron...

Article in *Journal of African Earth Sciences* · April 2016

DOI: 10.1016/j.jafrearsci.2016.04.016

CITATIONS

0

READS

44

1 author:



Adel Mady

Complutense University of Madrid

10 PUBLICATIONS 13 CITATIONS

SEE PROFILE

Some of the authors of this publication are also working on these related projects:



Mineralogy, Petrology and Genesis of Different Types of Ferromanganese Deposits [View project](#)

All content following this page was uploaded by [Adel Mady](#) on 25 April 2016.

The user has requested enhancement of the downloaded file. All in-text references [underlined in blue](#) are added to the original document and are linked to publications on ResearchGate, letting you access and read them immediately.

# Accepted Manuscript

Nummulite biostratigraphy of the Eocene succession in the Bahariya Depression, Egypt: Implications for timing of iron mineralization

A.M. Afify, J. Serra-Kiel, M.E. Sanz-Montero, J.P. Calvo, E.S. Sallam



PII: S1464-343X(16)30132-7

DOI: [10.1016/j.jafrearsci.2016.04.016](https://doi.org/10.1016/j.jafrearsci.2016.04.016)

Reference: AES 2552

To appear in: *Journal of African Earth Sciences*

Received Date: 2 February 2016

Revised Date: 14 April 2016

Accepted Date: 19 April 2016

Please cite this article as: Afify, A.M., Serra-Kiel, J., Sanz-Montero, M.E., Calvo, J.P., Sallam, E.S., Nummulite biostratigraphy of the Eocene succession in the Bahariya Depression, Egypt: Implications for timing of iron mineralization, *Journal of African Earth Sciences* (2016), doi: 10.1016/j.jafrearsci.2016.04.016.

This is a PDF file of an unedited manuscript that has been accepted for publication. As a service to our customers we are providing this early version of the manuscript. The manuscript will undergo copyediting, typesetting, and review of the resulting proof before it is published in its final form. Please note that during the production process errors may be discovered which could affect the content, and all legal disclaimers that apply to the journal pertain.

**Nummulite biostratigraphy of the Eocene succession in the Bahariya Depression,  
Egypt: Implications for timing of iron mineralization**

**Afify, A.M.<sup>a,b,\*</sup>, Serra-Kiel, J.<sup>c</sup>, Sanz-Montero, M.E.<sup>a</sup>, Calvo, J.P.<sup>a</sup>, Sallam, E.S.<sup>b</sup>**

a) Petrology and Geochemistry Department, Faculty of Geological Sciences, Complutense  
University, Madrid, C/ José Antonio Nováis, 2, 28040 Madrid, Spain

b) Geology Department, Faculty of Science, Benha University, 13518 Benha, Egypt

c) Stratigraphy, Paleontology and Marine Geosciences Department, University of Barcelona, C/  
Martí i Franquès, s/n, 08028 Barcelona, Spain

**\* Corresponding author ([adelmady@ucm.es](mailto:adelmady@ucm.es))**

**ABSTRACT**

In the northern part of the Bahariya Depression (Western Desert, Egypt) the Eocene carbonate succession, unconformably overlying the Cretaceous deposits, consists of three main stratigraphic units; the Naqb, Qazzun and El Hamra formations. The Eocene carbonates are relevant as they locally host a large economic iron mineralization. This work revises the stratigraphic attribution of the Eocene formations on the basis of larger benthic foraminifers from both carbonate and ironstone beds. Eight *Nummulites* species spanning the late Ypresian – early Bartonian (SBZ12 to SBZ17) were identified, thus refining the chronostratigraphic framework of the Eocene in that region of Central Egypt. Moreover, additional sedimentological insight of the Eocene carbonate rocks is presented. The carbonate deposits mainly represent shallow marine facies characteristic of inner to mid ramp settings; though deposits interpreted as intertidal to supratidal are locally recognized.

Dating of *Nummulites* assemblages from the youngest ironstone beds in the mines as early Bartonian provides crucial information on the timing of the hydrothermal and meteoric water processes resulting in the formation of the iron ore mineralization. The new data strongly support a post-depositional, structurally-controlled formation model for the ironstone mineralization of the Bahariya Depression.

Keywords: Nummulites, Eocene carbonates, ironstone, chronostratigraphy, Western Desert, Central Egypt.

## 1. Introduction

The Bahariya Depression is located near the central part of the Western Desert of Egypt (Fig. 1) where it shows elliptical geometry surrounded by a carbonate plateau mainly formed of Eocene rock units in its northern part. The Eocene stratigraphy, especially of the Middle to Upper Eocene formations in the Bahariya region has been a matter of dispute (Issawi et al., 2009). This was probably due to the lithostratigraphic variations and facies changes of the Eocene formations with respect to their equivalents outside the region as well as lack of agreement about the stratigraphic discontinuities between the exposed rock units in the area. Three Eocene rock units, the Naqb, Qazzun and El Hamra formations, were described exclusively for the Bahariya Depression by Said and Issawi (1964). These deposits have economic significance since they represent the host rock of the only ironstone mineralization currently exploited for steel industry in Egypt. Moreover, these ore deposits are unique along the Caenozoic palaeo-Tethyan shorelines in North Africa and South Europe (Salama et al., 2014) and can be interpreted as an analog for banded iron formations (BIFs) (Afify et al., 2015a, b). The origin of these deposits has also been a matter of scientific discussion for long time

(e.g., El Shazly, 1962; El Akkad and Issawi, 1963; Said and Issawi, 1964; Basta and Amer, 1969; [Dabous, 2002](#); Salama et al., 2013, 2014; Baioumy, 2014; Afify et al., 2014, 2015a, b). Despite this fact no much work was focused on the facies architecture and evolutionary pattern of the Eocene host rocks and their relation with the iron mineralization. Likewise, there is lack of detailed chronostratigraphic framework of the Eocene formations. In the classical papers on the geology of the region, e.g., Said and Issawi (1964), the age of the Naqb Formation was loosely attributed to the early Middle Eocene whereas the same rock unit was dated as upper Ypresian (middle Ilerdian-Cuisian) by Boukhary et al. (2011) on the basis of larger benthic foraminifera. The Qazzun Formation was attributed to the upper Middle Eocene without detailed biostratigraphic basis (Said and Issawi, 1964). This was also the case for El Hamra Formation, which was dated as Upper Eocene (Said and Issawi, 1964). In contrast, the stratigraphic review by Issawi et al. (2009) considered that the Lutetian is missing in the Bahariya Depression, which clearly points out a controversy on the chronostratigraphy of the Eocene rocks of the area.

This paper provides a scheme of the depositional and diagenetic features present in the Eocene carbonate formations cropping out in the northern part of the Bahariya Depression and aims to precise their chronostratigraphic framework. This is supported by new biostratigraphic evidence from larger benthic foraminifers collected from the carbonate and associated ironstone rocks. As a result, timing of the iron ore mineralization can be assessed more precisely.

## 2. Geologic setting

The sedimentary succession exposed at the northern part of the Bahariya area comprises the Cenomanian Bahariya Formation that is unconformably overlain by a

carbonate plateau formed of Eocene sediments (Fig. 1). The Eocene succession represented by the Naqb, Qazzun and El Hamra formations is truncated by Oligocene fluvial sandstone of the Radwan Formation (El Akkad and Issawi, 1963, Said and Issawi, 1964). The Bahariya Eocene rock units are equivalent to the Minia Fm. (= Naqb and Qazzun formations), Mokattam Fm. (= Rayan Fm.; = lower unit of the El Hamra Formation) and Maadi Fm. (= Qasr El Sagha Fm.; = upper unit of the El Hamra Fm.), which extend mostly to the north and north east of Egypt in the Nile Valley and Faiyum areas (Issawi et al., 1999). The Eocene carbonates in northern Bahariya are associated with ironstone mineralization, which affects these carbonate units at three main areas, i.e. El Gedida, Ghorabi and El Harra mines (Fig. 1) along two major fault systems (Afify et al., 2015b).

The Bahariya Depression was deformed by a NE-trending right-lateral wrench fault system associated with several doubly plunging folds and extensional faults (Fig. 1; Sehim, 1993; Moustafa et al., 2003). The strain regime in the Bahariya area was transpressional, starting by the end of the Campanian and being rejuvenated after the Eocene (Said and Issawi, 1964; Sehim, 1993; Moustafa et al., 2003). The post-Campanian NE-SW doubly plunging anticline folds and ENE strike-slip faults were continued throughout the Paleocene and early Eocene. Moreover, syndepositional tectonic activity and seismic pulses took place during deposition of the Eocene sediments (Said and Issawi, 1964). The depositional pattern of the Eocene rocks in the study area was controlled by a paleorelief sculpted in Late Cretaceous – Early Paleogene times, ultimately related to the rejuvenation of the Syrian Arc System (Said and Issawi, 1964). As a consequence, the carbonate succession was fractured and folded along NE to ENE oriented right-stepped en-échelon folds (Fig. 1). The faulting pattern

shows major NE-SW dextral strike-slip faults, WNW left-stepped, en-échelon normal faults, E-W normal faults and local thrusts (Fig. 1).

### 3. Materials and methods

Detailed fieldwork on the Eocene carbonate succession and the associated ironstone deposits was supported by analysis of satellite imagery (Figs. 1 and 2). Field observations and lithostratigraphic logging were complemented by collecting fossil specimens, especially larger benthic foraminifers (*Nummulites*), mainly from three outcrops (El Behour, Gar El Hamra and Teetotum Hill) as well as from the central part of El Gedida mine (Figs. 1 and 3). Altogether, we studied six samples collected from El Behour section (Figs. 1 and 3A), nine samples collected from Gar El Hamra section (four samples from the Qazzun Formation, five samples from the El Hamra Formation) (Figs. 1 and 3B), four samples from the Teetotum Hill section (Figs. 1 and 3C) and one sample from El Gedida mine section (Fig. 1). The soft samples with isolated *Nummulites* were disaggregated in a solution of  $\text{Na}_2\text{CO}_3$ ,  $\text{H}_2\text{O}_2$  and water and later sieved through apertures of 1.0, 0.5 and 0.2 mm. All the *Nummulites* samples are housed at the Stratigraphy, Paleontology and Marine Geosciences Department, University of Barcelona, Spain.

About 160 samples of carbonate, ironstone, sandstone, claystone and other rocks were collected during fieldwork. Indurated samples were prepared as thin sections and polished slabs. Petrography was carried out by using transmitted polarized and reflected light microscopes. Staining with alizarin red-potassium ferricyanide was used to differentiate the carbonate minerals. Scanning electron microscopic studies (SEM) were carried out for high-resolution textural and morphometric analyses. Fresh broken pieces were placed on sample holders supported by carbon conductive tape, followed by

sputter coating of gold and studied with a JEOL JSM-6400 operating at 20 kV and equipped with an energy dispersive X-ray microanalyzer (SEM-EDAX). Mineralogy for nearly all collected samples was verified by X-ray powder diffraction analyses (XRD) using a Philips PW-1710 diffractometer under monochromatic Cu K $\alpha$  radiation ( $\lambda=1.54060$  Å) operating at 40kv and 30 mA.

#### 4. Stratigraphy and sedimentology of the Eocene formations

The Eocene stratigraphic succession exposed at the northern Bahariya study area is sculptured geomorphologically as a carbonate plateau where superimposed cycles of weathering and erosion on these rock units resulted in formation of several geological landforms, e.g., mesas, buttes and conical hills (Fig. 1). Outcrops of the Naqb Formation can be traced along the western part of the study area (Fig. 1) where it is characterized by pinkish shading due to iron pigmentation and staining (Fig. 2A). Two sedimentary sequences separated by an irregular paleokarst surface can be differentiated in the Naqb Formation (Afify et al., 2015b) (Figs. 2B, C). The overlying Qazzun and El Hamra formations are well exposed to the north and east of the study area (Figs. 1 and 2A). The Qazzun Formation looks homogenous whilst the El Hamra Formation can be subdivided into two units; Lower Hamra and Upper Hamra (Figs. 2D and 3) (Issawi et al., 2009). The boundary between the two units of El Hamra Formation is marked by a brecciated, concretionary irregular thin calcareous bed cropping out at El Behour and Gar El Hamra sections (Figs. 3A, B). The Eocene rock units show features indicative of slight syndepositional folding forming anticline and syncline structures, especially around highly faulted areas (Fig. 1). In addition to the NW-SE fault systems affecting the Eocene carbonates, a major extensional NE fault system affected the study area (Fig.

1). These faults, with exposed length of tens of kilometers, likely developed in response to the Red Sea/Gulf of Suez rifting.

The Eocene marine carbonate formations are capped disconformably by an up to 20 m-thick succession of horizontally-bedded continental lacustrine carbonate deposits (Figs. 2A and 3). This unit (Continental carbonate unit) is described for the first time in the northern Bahariya area where it crops out with good exposure in the Teetotum and nearby hills (Fig. 1). This rock unit may be equivalent to the Miocene unit described by Pickford et al. (2010) in the center of the Bahariya Depression and to the post-Eocene deposits described by Sanz-Montero et al. (2013) in the adjacent Farafra Depression.

#### *4.1. Depositional and diagenetic features of the Eocene carbonate units*

Depositional features and palaeoenvironmental interpretation of the Eocene rock units are summarized in Table 1. Some additional insight about these formations is as follows:

##### *4.1.1. The Naqb Formation*

*Description:* The Naqb Formation overlies unconformably the Cenomanian Bahariya Formation and is overlain with seeming disconformity by the Qazzun Formation (Figs. 1 and 2A). The Naqb Formation at the Ghorabi and El Harra sections is up to 13 m thick. At those localities, the sedimentary succession consists mainly of dolostone and siliceous dolostone beds with few marlstone intercalations (Figs. 2B, C). The lower sequence of the Naqb Formation is mainly composed of nummulitic dolostone at the bottom (Fig. 4A), oolitic and fossiliferous dolostone at the middle part of the sequence (Fig. 4B; Table 1) and it is capped by fine- to medium-grained dolostone rocks (Fig. 4C). The upper sequence is composed of stromatolite-like, laminated (Figs. 4D, E),

fine-grained dolostone with scarce fossils (small sized, reworked foraminiferal tests). Laminated fenestral fabrics, stromatolite-like structure, evaporite pseudomorphs, desiccation cracks and rhizoliths are common features in the upper part of the Naqb Formation. This rock unit shows pervasive diagenetic features resulting from micritization (Fig. 4A), dolomitization (Fig. 4), silicification (Fig. 4B), stylolitization (Fig. 4C), dissolution (Fig. 4B) and cementation with pseudospherulitic, fibro-radiating carbonates (Fig. 4F). The latter process was mainly related to development of the paleokarst system that separates the two stratigraphic sequences.

*Interpretation:* The carbonate deposits of the Naqb Formation were accumulated in shallow depositional environments, from shallow subtidal to intertidal-supratidal (Afify et al., 2015b). The low diversity of fossil assemblages (e.g., nummulitids, alveolinids, textulariids, and dasycladacean algae) in the lower sequence could be interpreted as characteristic of oligophotic inner- to mid-ramp environments, preferably at water depth ranging from 40 to 80 m (Hottinger, 1997; Beavington-Penney and Racey, 2004) with random scatter of nutrients where the nummulitids preferred lower nutrient levels (Bassi et al., 2013). The association of nummulitids and alveolinids characterizes the shoals and banks of inner-ramp settings (Buxton and Pedley, 1989). In contrast, abundance of evaporite pseudomorphs, scarcity of fossils and calcretization in the upper sequence are indicative of high salinity, very shallow and calm conditions in intertidal-supratidal environments disturbed by current action (Warren, 2006; Ortí, 2010; Afify et al., 2015b).

#### 4.1.2. The Qazzun Formation

*Description:* The Qazzun Formation can be easily differentiated from the underlying and overlying Eocene rock units because of its distinctive chalky nature and bright

white color (Fig. 2A). Thickness of the Qazzun Formation ranges from 4 m at El Gedida area to 32.5 m at Gar El Hamra section (type section; Figs. 2D, 3B). The carbonate deposits of the Qazzun Formation consist mainly of massive, bright white, nummulite-rich chalky limestone forming tabular, meter-thick banks alternated with soft, slope-forming mud-supported chalky limestones. The carbonate rocks of the Qazzun Formation exhibit nummulitic wackestone and packstone fabrics where the nummulites tests occur usually scattered in the micrite matrix (Fig. 5A) although closely packed nummulites test are locally observed. Micritization and dissolution features are common.

*Interpretation:* The occurrence of nummulitic wackestone/packstone facies in banks with un-oriented fabrics reflects shallow water, high energy conditions in a middle ramp setting (Hottinger, 1997). The homogeneity of the facies forming the Qazzun Formation suggests low variation of sea-level through time.

#### 4.1.3. The El Hamra Formation

*Description:* Similar to the Qazzun Formation, the thickness of the El Hamra Formation increases towards the north where it reaches up to 65 m at Gar El Hamra section. The carbonate deposits of the El Hamra Formation are composed of soft to slightly indurated, fossil-rich limestone with sandy limestone, marlstone, glauconitic limestone, and siltstone intercalations. The formation is subdivided into two units separated by a thin discontinuous brecciated limestone bed (Lower Hamra and Upper Hamra; Figs. 2D, 3, Table 1). The lower unit is composed of yellow, massive, nummulite-rich limestone-sandy limestone beds with gradual upwards increase of oyster and gastropod banks (Fig. 3). Nummulitic packstone/rudstone, fossiliferous wackestone-packstone (Fig. 5B) and oyster rudstone (Fig. 5C) are the dominant facies in the Lower Hamra unit. Nummulitid

tests, miliolids, oyster and gastropod shells, coralline debris and echinoid spines are the most abundant fossil skeletons in the Lower Hamra unit (Table 1; Figs. 5B, C). The Upper Hamra unit is characterized by dominance of glauconitic fossiliferous sandy limestone, siltstone/sandy clays with gradual upward increase of clastics and gastropod and oyster banks (Figs. 2D, 3). These lithofacies are rich in silt-sized quartz grains and the terrigenous content can exceed 50% of the volume of the rock thus resulting in fossiliferous siltstone. The dominant facies of the Upper Hamra are the fossiliferous glauconitic packstone-grainstone (Fig. 5D), oyster rudstone and fossiliferous siltstone where the main skeletal particles are of oysters, gastropods, bryozoans and miliolids. Calcitization of skeletal particles, micritization and dissolution features are the main diagenetic features of the El Hamra Formation (Fig. 5B–D).

*Interpretation:* The carbonate and terrigenous facies of the El Hamra Formation are indicative of deep to shallow subtidal environments. The common occurrence of nummulite-rich banks in the lower unit reflects deep subtidal environment. The relative abundance of bioclasts in the Lower Hamra reflects different sub-environments, i.e. miliolids, gastropods and oysters live in the inner ramp environment whereas the nummulitids and echinoids are characteristic of deeper marine areas (Flügel, 2004). The Lower Hamra unit shows shallowing upward conditions enhanced by occurrence of oyster and gastropod banks in its upper part. The occurrence of brecciated deposits on the top of the lower unit points to an episode of subaerial exposure. The dominance of gastropod and oyster banks in the Upper Hamra unit indicates moderate to high energy conditions, lesser than 50 m deep, in nutrient-rich waters of inner ramp settings (Flügel, 2004). The abundance of silt-sized quartz grains and glauconitic grains in the packstone facies of the Upper Hamra unit typically reflects low sedimentation rate and deposition from suspension nearby a clastic source in shallow subtidal environments (Flügel,

2004). Prevalent shallow conditions in the Upper Hamra unit are consistent with a sea-level regression, as suggested by El Habaak et al. (2016).

#### 4.2. Sedimentary features of the ironstone mineralization

The Bahariya ironstone rocks are mainly located at three areas; i.e. the Ghorabi, El Harra and El Gedida mines. These locations are coincident with two major fault systems oriented NE-SW (Fig. 1). In the Ghorabi and El Harra areas, thickness of the ironstone succession ranges from 7 to 13 m, which is similar to the thickness of the carbonate deposits of the Naqb Formation in nearby areas. Likewise, the ironstone succession is formed of two sequences (Fig. 6A), where the iron-rich rocks show clear evidence for replacement and/or cementation of the carbonate fabrics by Fe-Mn minerals (Afify et al., 2015b). Some unaltered thin clay/marl beds occur intercalated with the ironstone rocks (Fig. 6A). At El Gedida mine, the ore mineralization consists of up to 30 m-thick black, indurated ironstone that comprehensively replaced the carbonate succession of the Eocene Naqb, Qazzun and El Hamra formations (Figs. 6B, 7). Most facies and fabrics occurring in the carbonate units were recognized in the ironstone. Towards the upper part of the ironstone succession in El Gedida, a 3 m-thick fossiliferous ironstone bed (Fig. 6B) furnished rich, well-preserved *Nummulites* assemblages. This bed is overlain by pisolithic ironstone rocks occurring at the topmost part of the ironstone succession. This is in turn is capped by up to 10 m-thick, greenish glauconitic claystone and up to 15 m-thick ferruginous black sandstone (the Radwan Formation) respectively (Fig. 6B). The green glauconitic beds are stratigraphically and sedimentologically correlatable with the upper unit of El Hamra Formation, despite it is barren of fossils.

A variety of minerals was determined in the ironstones, i.e. iron oxyhydroxides, quartz, manganese minerals, apatite, dolomite, clay minerals, and sulfate minerals (Afify et al., 2015b). Goethite and hematite are the main iron-bearing minerals. Petrography of the ironstone reveals that the ore deposits exhibit the main textures and structures of their precursor host carbonates (Fig. 8). The main textures and fabrics of the carbonates of the Naqb Formation are preserved in the ore deposits where nummulitic mud-wacke ironstone, oolitic and fossiliferous ironstone, massive to brecciated non-fossiliferous ironstone and stromatolite-like fabrics can be recognized (Fig. 8A–D). Likewise, the nummulitic wackestone-packstone facies characteristic of the Qazzun Formation and the fossiliferous packstone of the El Hamra Formation are recognizable in the ironstones (Figs. 8E, F). The topmost part of the ironstone succession includes large pisoids that show vadose cements (Figs. 8G, H) and some rhizoliths replaced by iron oxides (Fig. 8I). The association of vadose cements, pisoliths and root structures is clearly indicative of subaerial exposure.

Both the stratigraphic and structural features analyzed in the northern Bahariya area point to a close relationship between the distribution of the ironstone deposits and major faults (Figs. 1 and 7). Extensive replacement of the Eocene carbonate formations by Fe and Mn oxides and other associated minerals occurs in localized areas near major fault lineaments where the ore deposits retain largely many stratigraphic and sedimentary features of their host carbonate rocks, i.e. thickness, bedding, lateral and vertical sequential arrangement and fossil content. On basis of petrography, mineralogy and geochemistry as well as ironstone associations and distributions, Afify et al. (2014; 2015a, b) suggested that the iron oxyhydroxides were deposited in the carbonate rocks by hydrothermal solutions related to regional magmatic activity in the region and moved upwards through the NE-SW major faults, fractures and discontinuities.

## 4.3. Biostratigraphy of the Eocene formations and ironstones

The new biostratigraphic data provided in this work are based on the assemblages of *Nummulites*, a group of larger foraminifers well described and illustrated in monographs such as those by Schaub (1981, 1995) and Racey (1995). The biostratigraphic range of each species was determined according to zones defined by Schaub (1981) and the Shallow Benthic Zones (SBZ) characterized by Serra-Kiel et al. (1998). The species identified in this work are illustrated in Plate 1 and their biostratigraphic ranges are given in Figure 9. All data about the intervals and distribution of *Nummulites* in the studied sections are summarized in Figure 3, where the range chart of the 19 fossil samples is shown. All the *Nummulites* specimens were collected from the Qazzun and El Hamra formations. It was difficult to find well preserved specimens from the Naqb Formation in the studied sections due to the strong replacement of the fossil grains by silica. The sample collected from the upper part of the ironstone succession in the El Gedida mine (Fig. 6B) shows good preservation of *Nummulites* specimens with slight replacement by iron.

In the carbonate beds of the Qazzun Formation, at its type locality of Gar El Hamra section (Figs. 1 and 3B), three larger benthic foraminifers were identified, i.e. *Nummulites syrticus* SCHAUB, 1981 (Pl. 1, Fig. 26), *N. praelorioli* HERB & SCHAUB, 1963 (Pl. 1, Figs. 10–14) and *N. migiurtinus* AZZAROLI, 1952 (Pl. 1, Figs. 15–18). Likewise, four *Nummulites* species were identified from the carbonate deposits of the lower unit of the El Hamra Formation in the three studied sections (Fig. 3), i.e. *N. migiurtinus*, *N. gizehensis* (FORSKÅL, 1795) (Pl. 1, Figs. 1–9), *N. discorbinus* (SCHLOTHEIM, 1820) (Pl. 1, Figs. 27, 28) and *N. beaumonti* D'ARCHIAC & HAIME, 1853 (Pl. 1, Figs. 20, 21).

The carbonate beds of the upper unit of the El Hamra Formation are barren of *Nummulites* (Fig. 3), but contain diverse macrofossils such as *Ostrea clotbeyi*, *O. multicostata*, *Carolia placunoides* and *Turritella* sp.

A fossil sample collected from the uppermost part of the ironstone succession in the central hill of El Gedida mine (Figs. 1, 6B) yielded *Nummulites gizehensis*, *N. biarritzensis* D'ARCHIAC & HAIME, 1853 (Pl. 1, Fig. 25), *N. beaumonti* and *N. lyelli* D'ARCHIAC & HAIME, 1853 (Pl. 1, Figs. 29, 30).

The eight identified *Nummulites* species allow us to reassess the age of the Eocene rock units, especially the Qazzun and El Hamra formations. The distribution and time-span of these *Nummulites* species are shown in Figures 9 and 10. The presence of *Nummulites syrticus* and *N. praelorioli* in the lower part of the Qazzun Formation indicates an early Lutetian age (SBZ13) (Schaub, 1981; Serra-Kiel et al., 1998) whilst presence of *Nummulites migiurtinus* in the upper part of the Qazzun Formation and the lowermost part of the El Hamra Formation indicates an early to middle Lutetian age (SBZ13/SBZ14) (Schaub, 1981; Serra-Kiel et al., 1998). The dominance of *Nummulites gizehensis*, associated with *N. beaumonti* and *N. discorbinus* in the lower unit of the El Hamra Formation at Gar El Hamra and El Behour sections yields a middle-late Lutetian age (SBZ15/SBZ16) (Schaub, 1981; Serra-Kiel et al., 1998). The occurrence of *Nummulites beaumonti* in the upper part of the lower unit of the El Hamra Formation at the Teetotum Hill section suggests middle Lutetian (SBZ15) to Bartonian (SBZ17).

Summarizing, the Naqb Formation is considered to be middle-late Ilerdian in age because two *Nummulites* species, i.e. *Nummulites fraasi* DE LA HARPE, 1883 and *Nummulites pernotus* SCHAUB, 1951 (SBZ6 – SBZ9; Schaub, 1981; Serra-Kiel et al., 1998), were recorded in it by Boukhary et al. (2011) (Fig. 10). The *Nummulites* species studied from the Qazzun Formation assigned an early Lutetian age or SBZ13 for this

rock unit (Fig. 10). The lower unit of the El Hamra Formation is considered to be middle-late Lutetian/early Bartonian in age or SBZ14-SBZ17 (Fig. 10). Although no larger benthic foraminifers were collected by us from the upper unit of El Hamra Formation, it contains *Nummulites striatus* (BRUGUIÉRE, 1792) according to Issawi et al. (2009), indicating the Bartonian-early Priabonian or SBZ18-SBZ19 (Fig. 10).

Unfortunately, the low diversity of *Nummulites* -only eight species have been identified- does not permit greater precision between the boundaries of the Shallow Benthic Zones (SBZs).

## 5. Discussion on timing of ore mineralization processes

The close similarities of both lithostratigraphic and sedimentary features between the ironstone and the Eocene carbonate formations in which the ironstone is hosted strongly support replacement and cementation of the carbonates by silica, iron oxyhydroxides, manganese-rich and other subordinate minerals as a result of post-depositional and structurally-controlled processes. This was clearly demonstrated by Afify et al. (2015b) for the dolostones of the Naqb Formation. Moreover, recognition of replacement and/or cementation of the carbonate deposits of the Qazzun and El Hamra formations by the same assemblage of Fe-Mn minerals strongly suggests that the whole set of Eocene deposits were affected by a unique hydrothermal event sourcing iron-rich fluids. These fluids moved throughout the main fault systems that affected the Eocene carbonate formations (Fig. 7) and mixed with meteoric groundwater (Afify et al., 2015a) so that relative timing for the precipitation of the iron ore minerals must be linked to the deformational stages of the Eocene carbonate plateau. Fault zones played a crucial role in focusing fluid migration into the basin, as can be inferred from the study of many hydrothermal, sediment-hosted ore deposits worldwide (Ceriani et al., 2011).

The lateral association of the ironstone mineralization with volcanic rocks south of the study area argues for the relationship between the formation of the ironstone and magmatism (Afify et al., 2014; 2015a, b).

The ironstone deposits were formed through dissolution-corrosion of the host carbonate rocks with no replacement of the associated clay intercalations. The widespread red pigmentation of the carbonate deposits of the Naqb Formation by comparison to those of the Qazzun and El Hamra formations was favored by the more porous fabrics of the dolostones, i.e. dolostone is more porous and susceptible to fracturing and brecciation than limestone (Budd and Vacher, 2004). The replacement was most probably syngenetic to the formation of the pisolithic fabrics on the topmost part of the ironstone succession and before the deposition of the glauconitic claystone overburden that was not affected by iron mineralization. Altogether, the aforementioned deformational and karstic features determined the morphology and extent of alteration and mineralization exposed in the area and enhanced by permeability of carbonate rocks.

The new biostratigraphic data acquired in this paper allows integration of the post-depositional genetic model proposed previously by Afify et al. (2015a, b) for the ironstone deposits with the chronology of the ore-forming processes. The presence of ferruginized specimens of *N. gizehensis* (SBZ14–SBZ16), *N. beaumonti* (SBZ15–SBZ17), *N. lyelli* (SBZ17) and *N. biarritzensis* (SBZ17) of middle-late Lutetian/Bartonian age in the upper part of the ironstone succession at El Gedida mine area along with the presence of alveolinids and nummulitids of the Naqb Formation and the nummulitids of the Qazzun Formation indicates that the carbonates replaced by the ore deposits span late Ypresian – early Bartonian. The formation of the ore deposits can be dated later than early Bartonian, most probably during the Priabonian and before the

Oligocene which is supported by the fact that neither the Priabonian glauconitic claystones related to the upper unit of the El Hamra Formation nor the Oligocene sandstones show iron replacement. This statement is consistent with the Late Eocene magnetization assigned for the Bahariya area by Odah (2004) and confirms previous interpretation by Afify et al. (2015b) that the ironstone was a post-depositional, structurally-controlled ore deposit.

## 6. Concluding remarks

The chronostratigraphy of the Eocene rock units forming the carbonate plateau to the north of the Bahariya Depression (Western Desert) has been precised by analyzing new samples of *Nummulites* species collected in the study area. The Naqb Formation is dated as middle to late Ilerdian (late Ypresian; SBZ6 to SBZ9) whilst the Qazzun Formation contains fauna attributable to the early Lutetian (SBZ13). On the basis of larger benthic foraminifers, the lower unit of the El Hamra Formation is dated as middle to late Lutetian (SBZ14 to SBZ16) reaching up to the early Bartonian (SBZ17) whereas the age of the upper unit is attributed to the late Bartonian and part of the Priabonian as indicated by mollusk assemblages. According to this data, the Lutetian stage is identified for the first time in the region. Moreover, the succession exposed in the northern Bahariya shows a rather long record of Eocene strata.

Dating of *Nummulites* assemblages from the youngest ironstone beds as early Bartonian gives light on the relative timing for the hydrothermal and meteoric groundwater processes that led to the formation of the ore body. These processes probably took place throughout the Priabonian. At that time, sea level regression resulted in subaerial exposure ultimately related to tectonic deformation of the region.

Ascending hydrothermal fluids leading to the formation of the ore minerals followed the pathways created by the fault systems affecting the area.

## Acknowledgements

We would like to thank Dr. Juan Pablo Rodríguez-Aranda for helping in drawing figures and revising the manuscript. The authors are indebted to Editor-In-Chief of Journal of African Earth Sciences, for reviewing and editing of the manuscript. Special thanks to Prof. Dr. Johannes Pignatti, Roma University, and an anonymous reviewer for their encouraging comments and annotations that greatly improved an earlier version of the manuscript. This project was financially supported by the Egyptian Government in a full fellowship to the first author at Complutense University of Madrid, Spain. This work is a part of the activities of Research Groups BSHC UCM-910404 and BSHC UCM-910607 and part of the project CGL2015-60805-P on the biostratigraphy of the Paleogene led by Carles Martin Closas, Barcelona University.

## References

- Afify, A.M., Arroyo, X., Sanz-Montero, M.E., Calvo, J.P., 2014. Clay mineralogy in Bahariya area, Egypt: Hydrothermal implications on fault-related iron ore deposits, 7th Mid European Clay Conference, Germany, Abstract, pp. 137.
- Afify, A.M., González-Acebrón, L., Sanz-Montero, M.E., Calvo, J.P., 2015a. Unravelling the origin of Bahariya ironstone of Egypt. ECROFI XXIII Conference (The Sorby Conference on Fluid and Melt Inclusions), United Kingdom, Abstract, pp. 136–137.
- Afify, A.M., Sanz-Montero, M.E., Calvo, J.P., 2015b. [Ironstone deposits hosted in Eocene carbonates from Bahariya \(Egypt\) - New perspective on cherty ironstone occurrences. Sedimentary Geology 329, 81–97.](#)
- Baioumy, H.M., Ahmed H. H., Mohamed Z. K., 2014. A mixed hydrogeneous and hydrothermal origin of the Bahariya iron ores, Egypt: Evidences from the trace and rare earth elements geochemistry. Journal of Geochemical Exploration 146, 149–162.
- Bassi, D., Nebelsick, J.H., Puga-Bernabéu, Á., Luciani, V., 2013. Middle Eocene Nummulites and their offshore re-deposition: A case study from the Middle Eocene of the Venetian area, northeastern Italy. Sedimentary Geology 297, 1–5.
- Basta, E.Z., Amer, H.I., 1969. El Gedida iron ores and their origin, Bahariya oasis, Western Desert, U.A.R. Economic Geology 64, 424–444.

- 453 Beavington-Penney, S.J., Racey, A., 2004. Ecology of extant nummulitids and other larger benthic  
454 foraminifera: applications in palaeoenvironmental analysis. *Earth-Science Reviews* 67, 219–265.
- 455 Boukhary, M., Hussein-Kamel, Y., Abdelmalik, W. Besada, M., 2011. Ypresian nummulites from the  
456 Nile Valley and the Western Desert of Egypt: their systematic and biostratigraphic significance.  
457 *Micropaleontology* 571, 1–35.
- 458 [Budd, D.A., Vacher, H.L. 2004. Matrix permeability of the confined Floridan Aquifer, Florida, U.S.A.](#)  
459 *Hydrogeology Journal* 12, 531–549.
- 460 [Buxton, M.W.N., Pedley, H.M., 1989. Short paper: A standardized model for Tethyan Tertiary carbonate](#)  
461 [ramps. \*Journal of the Geological Society, London\* 146, 746–748.](#)
- 462 Ceriani, A., Calabró, R., Di Giulio, A., Buonaguro, R., 2011. Diagenetic and thermal history of the  
463 Jurassic-Tertiary succession of the Zagros Mountains in the Dezful Embayment (SW Iran):  
464 constraints from fluid inclusions. *International Journal of Earth Sciences* 100, 1265–1281.
- 465 [Dabous, A.A., 2002. Uranium isotopic evidence for the origin of the Bahariya iron deposits, Egypt. \*Ore\*](#)  
466 [Geology Reviews 19, 165–186.](#)
- 467 El Akkad, S.E., Issawi, B., 1963. Geology and iron ore deposits of Bahariya Oasis. *Geological Survey of*  
468 *Egypt* 18, 300 pp.
- 469 El Habaak, G., Askalany, M., Galal, M., Abdel-Hakeem, M., 2016. Upper Eocene glauconites from the  
470 Bahariya depression: An evidence for the marine regression in Egypt. *Journal of African Earth*  
471 *Sciences* 117, 1–11.
- 472 El Shazly, E.M., 1962. Report on the results of drilling in the iron ore deposit of Gebel Ghorabi, Bahariya  
473 Oasis, Western Desert. *Geological Survey of Egypt*, 25 p.
- 474 [Flügel, E., 2004. \*Microfacies of Carbonate Rocks: Analysis, Interpretation and Application\*. Springer,](#)  
475 [Berlin, 976 p.](#)
- 476 Hottinger, L., 1997. Shallow benthic foraminiferal assemblages as signals for depth of their deposition  
477 and their limitations. *Bulletin de la Société géologique de France* 168, 491–505.
- 478 [Issawi, B., El Hinnawi, M., Francis, M. and Mazhar, A., 1999. The Phanerozoic geology of Egypt; a](#)  
479 [geodynamic approach. Egyptian Geological Survey, Special publication No. 76. 462p.](#)
- 480 Issawi B, Francis M, Youssef A, Osman R 2009. The Phanerozoic of Egypt: a geodynamic approach.  
481 *Egyptian Geological Survey, Special publication No. 81, 589p.*
- 482 Moustafa, A.R., Saoudi, A., Moubasher, A., Ibrahim, I.M., Molokhia, H., Schwartz, B., 2003. Structural  
483 setting and tectonic evolution of the Bahariya Depression, Western Desert, Egypt. *GeoArabia*  
484 8(1), 91–124.
- 485 Odah, H., 2004. Paleomagnetism of the Upper Cretaceous Bahariya Formation, Bahariya Oasis, Western  
486 Desert, Egypt. *Journal of Applied Geophysics* 3(2), 177–187.
- 487 Ortí, F., 2010. Evaporitas: introducción a la sedimentología evaporítica, In: Arche, A. (Ed.),  
488 *Sedimentología. Del Proceso Físico a la Cuenca Sedimentaria*. Consejo Superior de  
489 *Investigaciones Científicas, Madrid, 675–769.*
- 490 Pickford, M., Wanas, H.A., Mein, P., Ségalen, L., Soliman, H., 2010. The extent of paleokarst and fluvio-  
491 lacustrine features in the Western Desert, Egypt; Late Miocene subaerial and subterranean  
492 paleohydrology of the Bahariya–Farafrá area. *Bulletin of the Tethys Geological Society, Cairo,*  
493 *Egypt* 5, 35–42.
- 494 Racey, A., 1995. Lithostratigraphy and larger foraminiferal (nummulitid) biostratigraphy of the Tertiary  
495 of northern Oman. *Micropaleontology*, 41, 123p.
- 496 Said, R., Issawi, B., 1964. Geology of the northern plateau, Bahariya Oasis, Egypt. *Geological Survey of*  
497 *Egypt* 29, 41 pp.

- Salama, W., El Aref, M.M., Gaupp, R. 2013. Mineral evolution and processes of ferruginous microbialite accretion – an example from the Middle Eocene stromatolitic and ooidal ironstones of the Bahariya Depression, Western Desert, Egypt. *Geobiology* 11, 15–28.
- Salama, W., El Aref, M.M., Gaupp, R. 2014. Facies analysis and palaeoclimatic significance of ironstones formed during the Eocene greenhouse. *Sedimentology* 61, 1594–1624.
- Sanz-Montero, M.E., Wanas, H., Muñoz-García, M.B., González-Acebrón, L., López, M.V., 2013. The uppermost deposits of the stratigraphic succession of the Farafra Depression (Western Desert, Egypt): Evolution to a Post-Eocene continental event. *Journal of African Earth Sciences* 87, 33–43.
- Schaub, H. 1981. Nummulites et Assilines de la Tethys paléogène. Taxinomie, phylogénese et biostratigraphie. *Mémoires suisses de Paléontologie*, 104, 236 p., 105 and 106, 97p.
- Schaub, H. 1995. Nummulites of Israel. In: *The Biostratigraphy of the Eocene of Israel* H. Schaub, C. Benjamini & S. Moshkovitz eds. *Mémoires suisses de Paléontologie*, 11, 19–32, 12 plates.
- Sehim, A.A., 1993. Cretaceous tectonics in Egypt. *Egyptian Journal of Geology* 371, 335–372.
- Serra-Kiel, J., Hottinger, L., Caus, E., Drobne, K., Ferràndez, C., Jauhri, A.K., Less, G., Pavlovec, R., Pignatti, J., Samsó, J.M., Schaub, H., Sirel, E., Strougo, A., Tambareau, Y., Tosquella, J. and Zakrevskaya, E. 1998. Larger foraminiferal biostratigraphy of the Tethyan Paleocene and Eocene. *Bulletin de la Société géologique de France*, 169 (2), 281-299.
- Warren, J.K., 2006. *Evaporites: Sediments, Resources and Hydrocarbons*: Springer, Berlin, 1035p.

**TABLE CAPTIONS**

**Table 1.** Summary of the sedimentary features, fossil content and palaeoenvironments for the three Eocene formations in the northern Bahariya region.

**FIGURE CAPTIONS**

**Fig. 1.** Geologic map of the northern Bahariya area (modified after Said and Issawi, 1964). See locations of the measured sections.

**Fig. 2.** A. Landsat image showing the distribution of the Eocene rock units through the northern part of the Bahariya area (1- Naqb Formation, 2- Qazzun Formation and 3- El Hamra Formation). Note that the Eocene formations are overlain unconformably by nearly horizontal continental carbonate unit (4). B. Columnar section showing the two sequences of the Naqb Formation at the section studied at Ghorabi area. C. Outcrop view showing the two sequences (1: lower sequence, 2: upper sequence) of the Naqb Formation separated by paleokarst features. D. Field photograph showing the type section of the Qazzun and El Hamra formations at Gar El Hamra area.

**Fig. 3.** Stratigraphic cross-section showing the distribution of *Nummulites* along the El-Behour section (A), the Gar El Hamra section (B) and the Teetotum Hill section (C).

**Fig. 4.** Petrographic features of the Naqb Formation. A. Nummulitic dolostone with medium-grained dolomite rhombs. Note the partial dissolution of the dolomite crystals as well as the micritization of the nummulitid tests. B. Oolitic fossiliferous dolostone showing dissolution pores cemented by quartz. C. Fine to medium grained dolostone. Note a vertical stylolite cemented by calcite (arrow). D, E. Stromatolite-like dolostone. Note the white laminae of quartz in-between the fine laminae of dolomites (D) with desiccation cracks (E). F. Pseudospherulitic and fibro-radiating dolomite after calcite. All microphotographs in crossed nicols (C.N.).

**Fig. 5.** Textures of the Qazzun and El Hamra formations. A. Nummulitic wackestone/packstone facies with nummulitid tests scattered in the micritic matrix (C.N.). B. Fossiliferous packstone with nummulitid tests, gastropods, oysters and miliolids closely packed together. Note the calcitization of the skeletal particles (C.N.).

C. Oyster rudstone with shells commonly bored (C.N.). D. Glauconitic fossiliferous packstone with bivalve shell fragments, gastropods, miliolids and oxidized glauconitic grains (PPL). (C.N. = crossed nicols, PPL = plane polarized light).

**Fig. 6.** A. Panoramic view of the Naqb Formation showing ironstone beds and clay intercalations (white arrows) arranged in two sequences. B. Outcrop view of the ironstone succession exposed at the central part of El Gedida mine (X is the location of the collected fossil sample).

**Fig. 7.** Landsat image showing the main exploited ore mine of El Gedida and the surrounding carbonates. The geologic profile shows the structural and stratigraphic relationships of the Eocene units and the ore deposits in the same area.

**Fig. 8.** Microphotographs showing different ironstone fabrics: A. Nummulitic ironstone with quartz cementing moldic porosity (C.N.). B. Oolitic, fossiliferous ironstone where all the grains are partly replaced/cemented by iron and quartz after dolomite (C.N.). C. Highly crenulated, colloform ferromanganese oxides replacing speleogenic carbonates (PPL). D. Laminated iron with high porosity in-between the laminae (PPL). E. Ghosts of nummulitid tests scattered in iron oxide groundmass, Qazzun Formation (PPL). F. Fossiliferous ironstone with nummulitic tests and some fragmented bivalve shells replaced by iron as well as quartz, El Hamra Formation (C.N.). G, H. Pisolithic ironstone with irregular pisoliths packed together and cemented by fibrous and microcrystalline iron cement (G. PPL, H. reflected light). I. SEM photo showing tabular hematite replacing rootlets in the pisolithic ironstone.

**Fig. 9.** *Nummulites* species identified in the Qazzun and El Hamra formations and their biostratigraphic range according to Schaub (1981) and Serra-Kiel et al. (1998).

**Fig. 10.** A composite section (not at scale) of the main Eocene lithostratigraphic and chronostrigraphic units and shallow benthic foraminiferal zones (SBZs) after Serra-Kiel

et al. (1998). The shallow benthic zones written in red color are re-interpreted after previous dating by Boukhary et al. (2011) and Said and Issawi (1964). The violet shaded rectangle is the relative timing proposed for the iron mineralization.

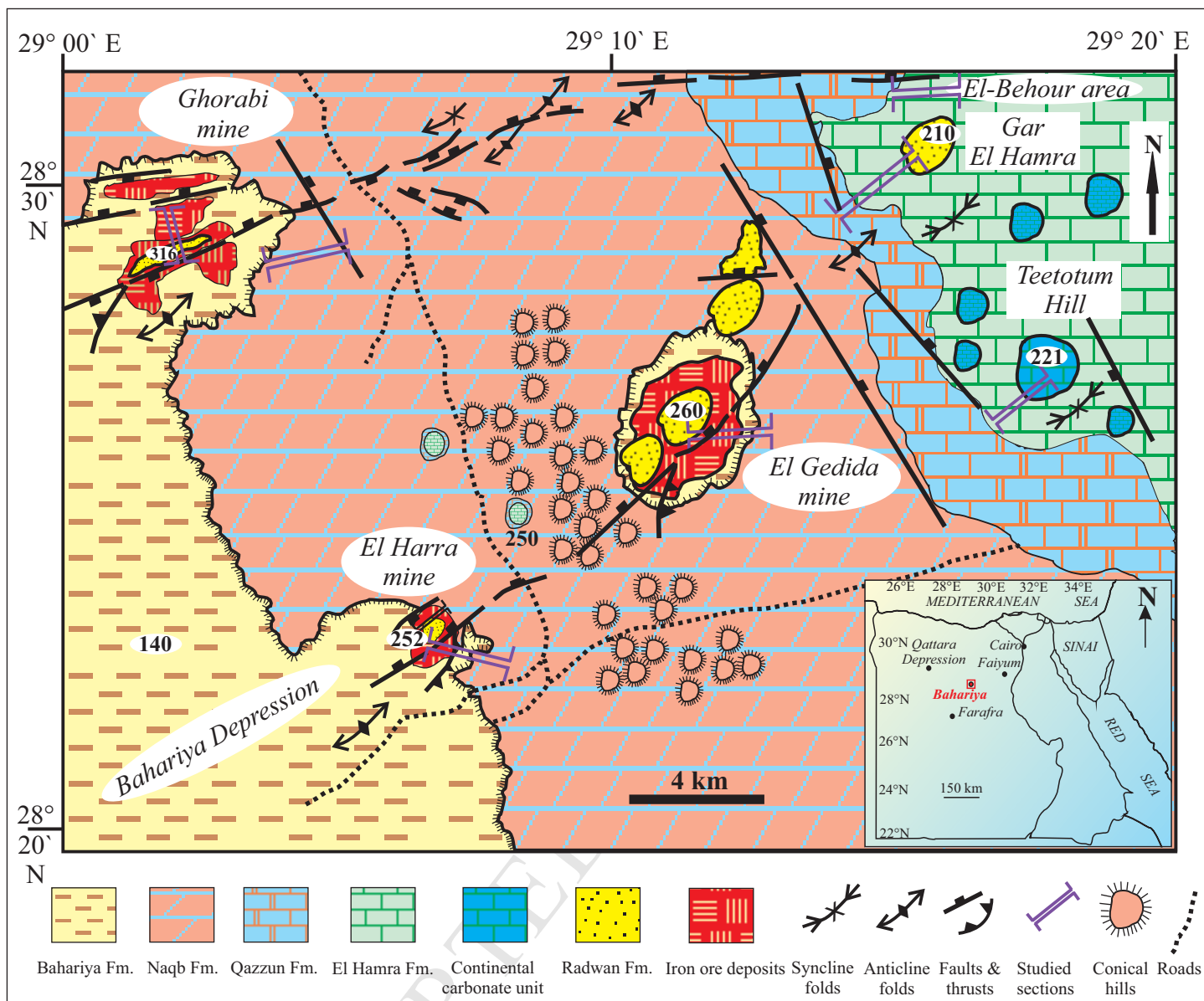
**PLATE CAPTIONS**

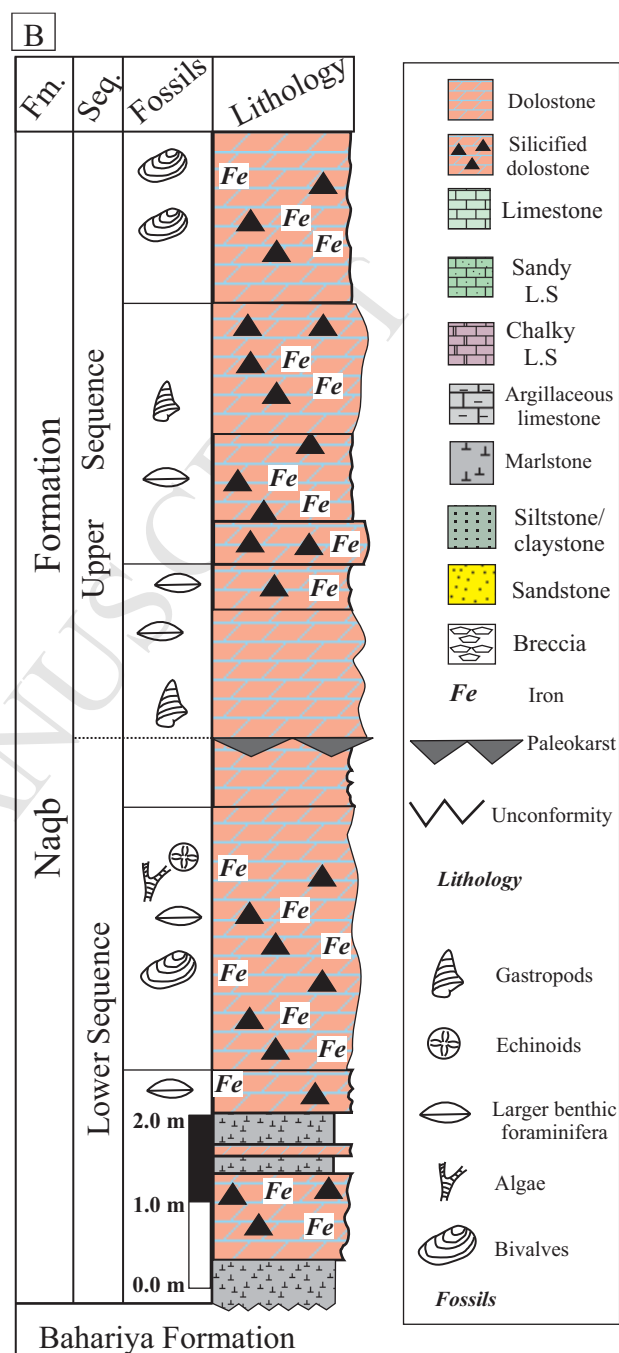
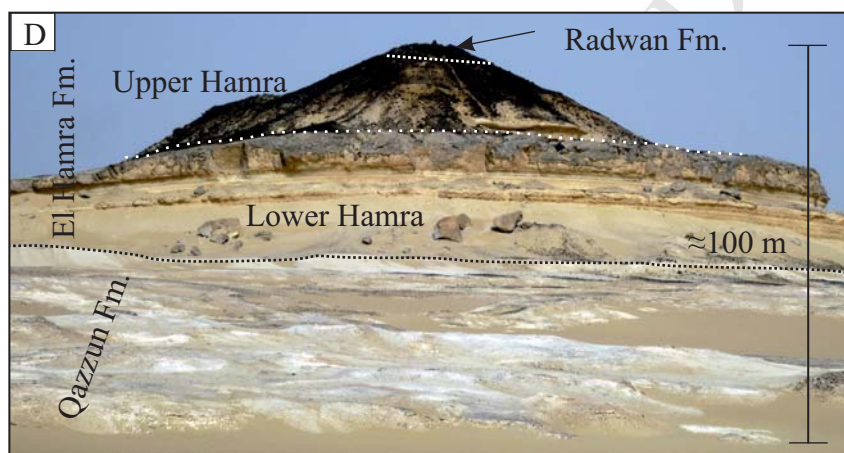
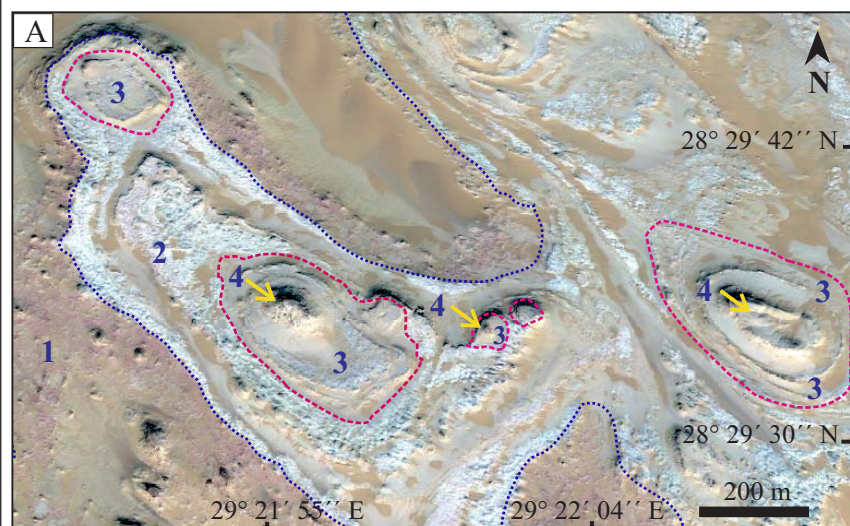
**Plate 1.**

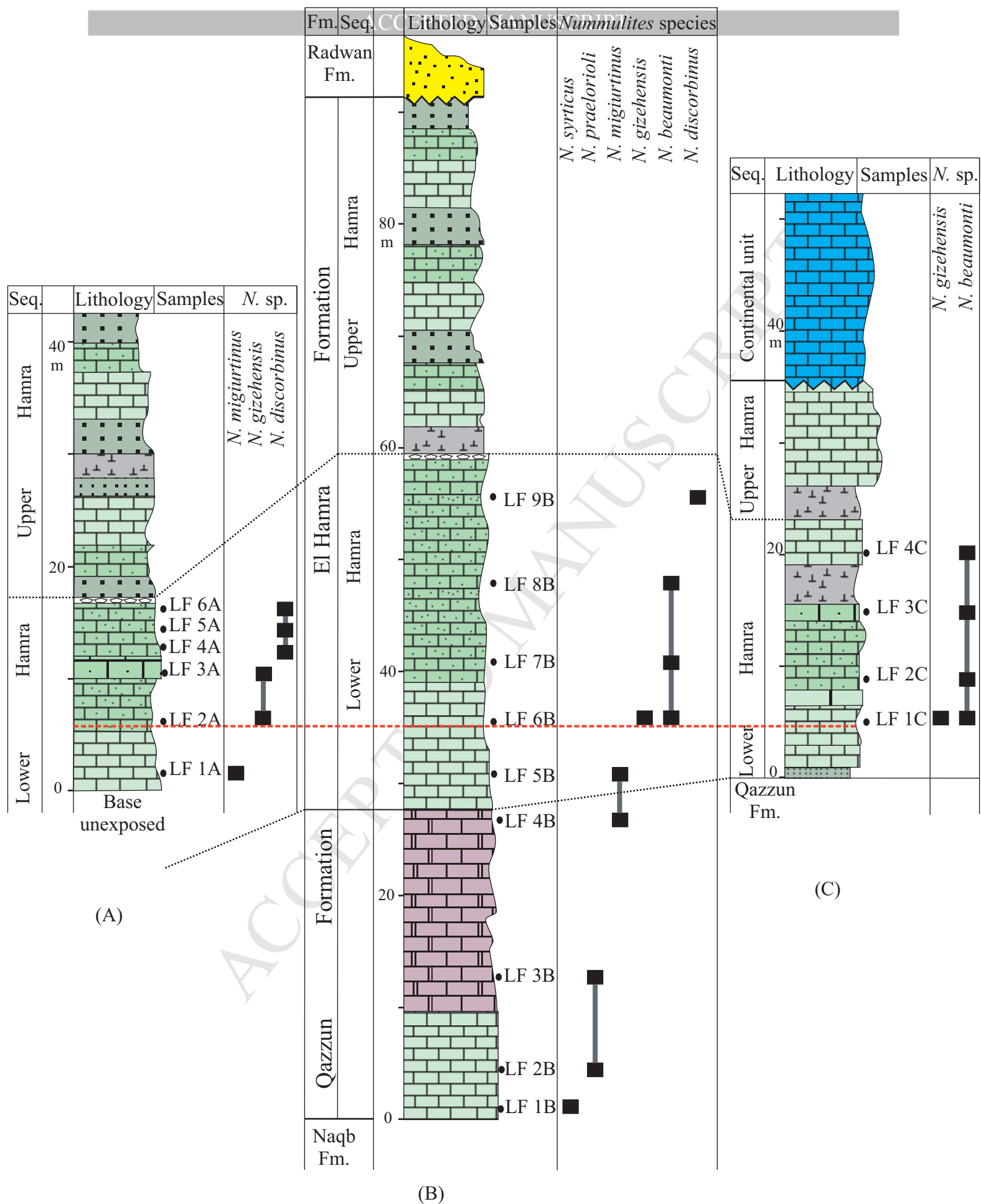
**1–9: *Nummulites gizehensis* (FORSKÅL, 1795)** 1–7 megalospheric forms; 8–9 microspheric forms; 1, 3, 5, 6 and 8 equatorial sections; 2, 4, 7 and 9 external views. Specimens 1, 2, 5–9 from sample LF 6B; 3 and 4 from sample LF 2A. **10–14: *Nummulites praelorioli* HERB & SCHAUB, 1963;** 10–13 microspheric forms; 14 megalospheric form. All specimens are equatorial sections. Specimens 10, 11 and 14 from sample LF 3B; 12 and 13 from sample LF 2B. **15–18: *Nummulites migiurtinus* AZZAROLI, 1952** 15–17 microspheric forms; 18 megalospheric form; 15, 16 and 18 equatorial sections; 17 external view. All specimens from sample LF 4B. **19–24: *Nummulites beaumonti* D’ARCHIAC & HAIME, 1853;** 19–21 microspheric forms; 22–24 megalospheric forms; 19, 21–24 equatorial sections; 20 external view. Specimens 19–21 from sample LF 1C; 22–23 from sample LF 8B and 24 from sample LF 7B. **25: *Nummulites biarritzensis* D’ARCHIAC & HAIME, 1853;** microspheric form; equatorial section. Specimen from El Gedida ironstone sample. **26: *Nummulites syrticus* SCHAUB, 1981;** microspheric form; equatorial section. Specimen from sample LF 1B. **27–28: *Nummulites discorbinus* (SCHLOTHEIM, 1820);** microspheric forms, 27 equatorial section; 28 external view. Specimens from sample LF 9B. **29–30: *Nummulites lyelli* D’ARCHIAC & HAIME, 1853;** megalospheric forms; 29 equatorial section; 30 external view. Specimen from El Gedida ironstone sample.

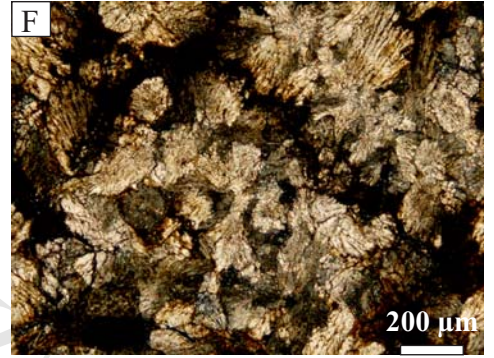
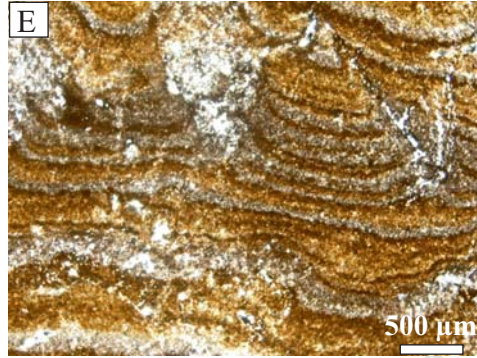
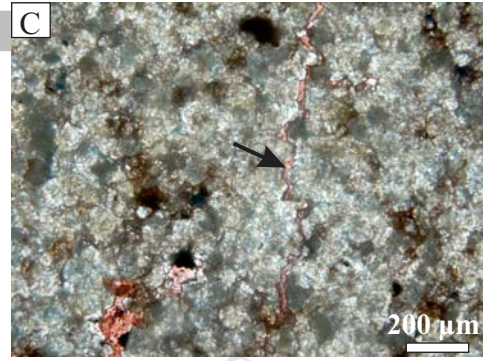
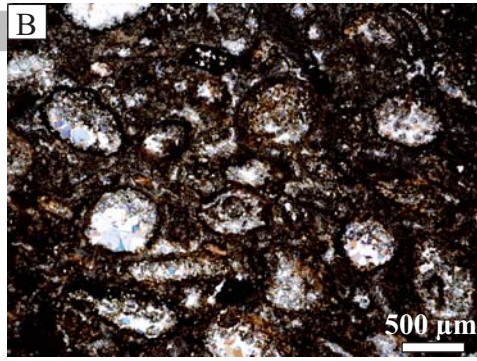
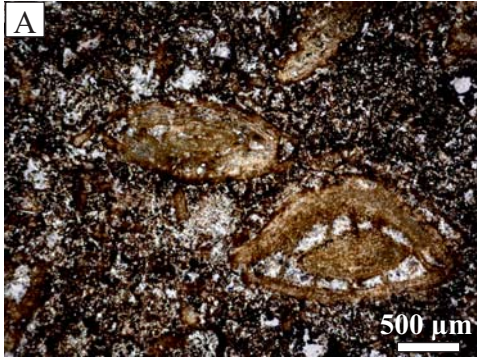
Lithostratigraphic units		Sedimentary facies	Petrography	Palaeoenvironments
El Hamra Formation	Upper Hamra	Slightly-indurated sandy limestone and glauconitic limestone beds are intercalated with fossiliferous siltstone/claystone beds. Sandy and silty grains in the limestone beds are more abundant to the top. The carbonate beds form banks of macrofossils. <i>Fossil content</i> – barren of <i>Nummulites</i> , but rich in macrofossils, e.g. <i>Ostrea clotbeyi</i> , <i>O. multcostata</i> , <i>Carolia placunoides</i> , and <i>Turritella</i> sp.	Sandy glauconitic packstone, fossiliferous siltstone and oyster rudstone are common.	Abundance of sandy and silty detrital grains as well as occurrence of glauconite grains altogether with the fossil grains reflects shallow water near the clastic source in restricted lagoonal environments.
	Lower Hamra	Bedded to massive limestone locally showing flat to concave-up, reef-like structure. Indurated to friable limestone beds include few marl interbeds. Coralline debris and burrows are common. <i>Fossil content</i> - high faunal diversity, i.e. <i>Nummulites</i> ( <i>N. migiurtinus</i> , <i>N. gizehensis</i> , <i>N. discorbinus</i> , <i>N. beaumonti</i> ), oysters ( <i>Ostrea clotbeyi</i> , <i>O. multcostata</i> , <i>Carolia placunoides</i> ), gastropods (e.g. <i>Turritella</i> sp.), and echinoid spines.	Variety of carbonate fabrics with variable skeletal grains including fossiliferous (namely nummulitic) packstone, bivalve (namely oysters) rudstone, fossiliferous packstone/grainstone.	Deposition in inner to middle ramp settings of moderate to high energy, as indicated by occurrence of banks of abraded nummulitid tests, coralline debris, gastropod shells, and oysters showing grain (but matrix-bearing)-supported carbonate fabrics.
Qazzun Formation		Homogeneous chalky limestone showing characteristic snow whitish color at large outcrop scale. Boundaries between the chalky limestone beds are not well defined and internal structure is mostly massive. <i>Fossil content</i> - nummulitids ( <i>Nummulites praelorioli</i> , <i>N. syrticus</i> and <i>N. migiurtinus</i> ).	Carbonate fabrics are homogeneous and comprise mainly nummulitic wackestone with minor occurrence of grain-supported carbonate.	Deposition in a low-energy middle ramp setting as indicated by lack of tractive sedimentary structures, low abrasion of the nummulitid tests, and abundance of mud-supported carbonate fabrics.
		Thick-bedded dolostone overlain by	Stromatolite-like laminated	Deposition in intertidal to

Naqb Formation	Upper sequence	stromatolite-like laminated dolostone. Cross-bedded bivalve dolostone at the top. Local occurrence of desiccation cracks, rhizoliths and bioturbation tubes. <i>Fossil content</i> - scarcity of fossils, mainly small reworked nummulitid tests. Bivalves are abundant in the uppermost part of the sequence where they occur as densely-packed bivalve shells.	dolostone formed of mudstone to wackestone with scattered bioclasts. Local occurrence of pseudo-morphs of evaporite crystals replaced by quartz. Bivalve-rich beds show wackestone to packstone fabrics, the bivalve shell being silicified and/or calcitized.	supratidal environments undergoing episodic desiccation and high salinity conditions, which resulted in formation of evaporite minerals and development of exposure features. These conditions are also indicated by very low faunal diversity together with small size of the foraminifer tests.
	Lower sequence	Variety of sedimentary facies including thinly-bedded dolostone/marly dolostone, cross-bedded oolitic and fossiliferous dolostone, and massive non-fossiliferous dolostone. <i>Fossil content</i> - nummulitids, bivalve and gastropods dominant at the base of the sequence whilst dasyclads, nummulitids, and alveolinids are abundant in the middle/upper part of the sequence.	Carbonate fabrics are varied concomitantly with the variety of sedimentary facies. Bioclastic packstone and oolitic grainstone abound in the middle part of the sequence. Silicification, i.e. replacement and/or cementation by quartz of the carbonate grains is common.	Deposition of the carbonate sediments of the lower sequence took place in a lagoon – inner shelf environment with development of moderate-to-high energy bioclastic and oolitic shoals. This environment became progressively shallow until complete exposure and further development of a paleokarst.

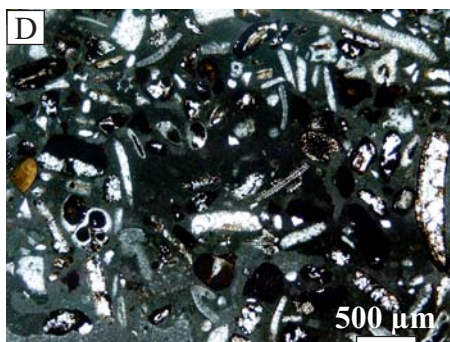


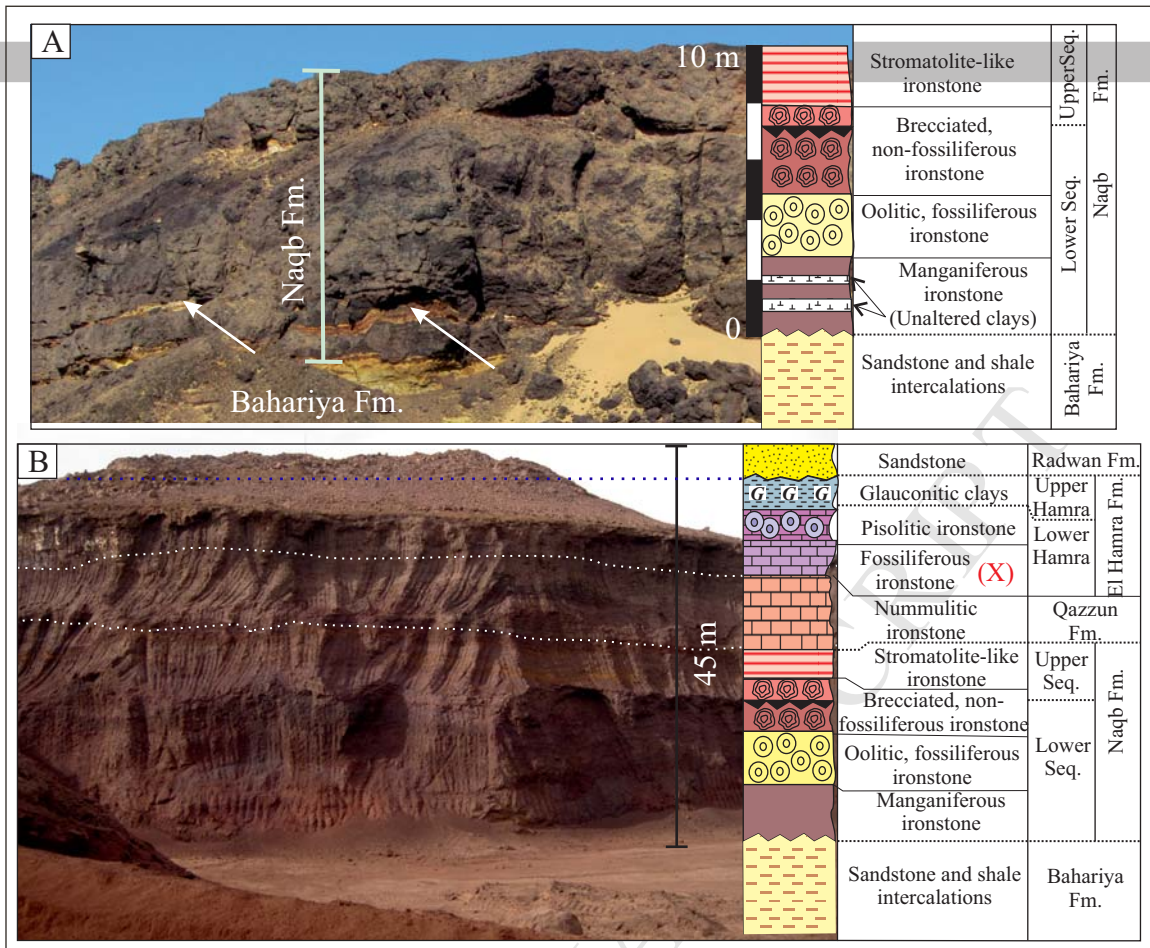


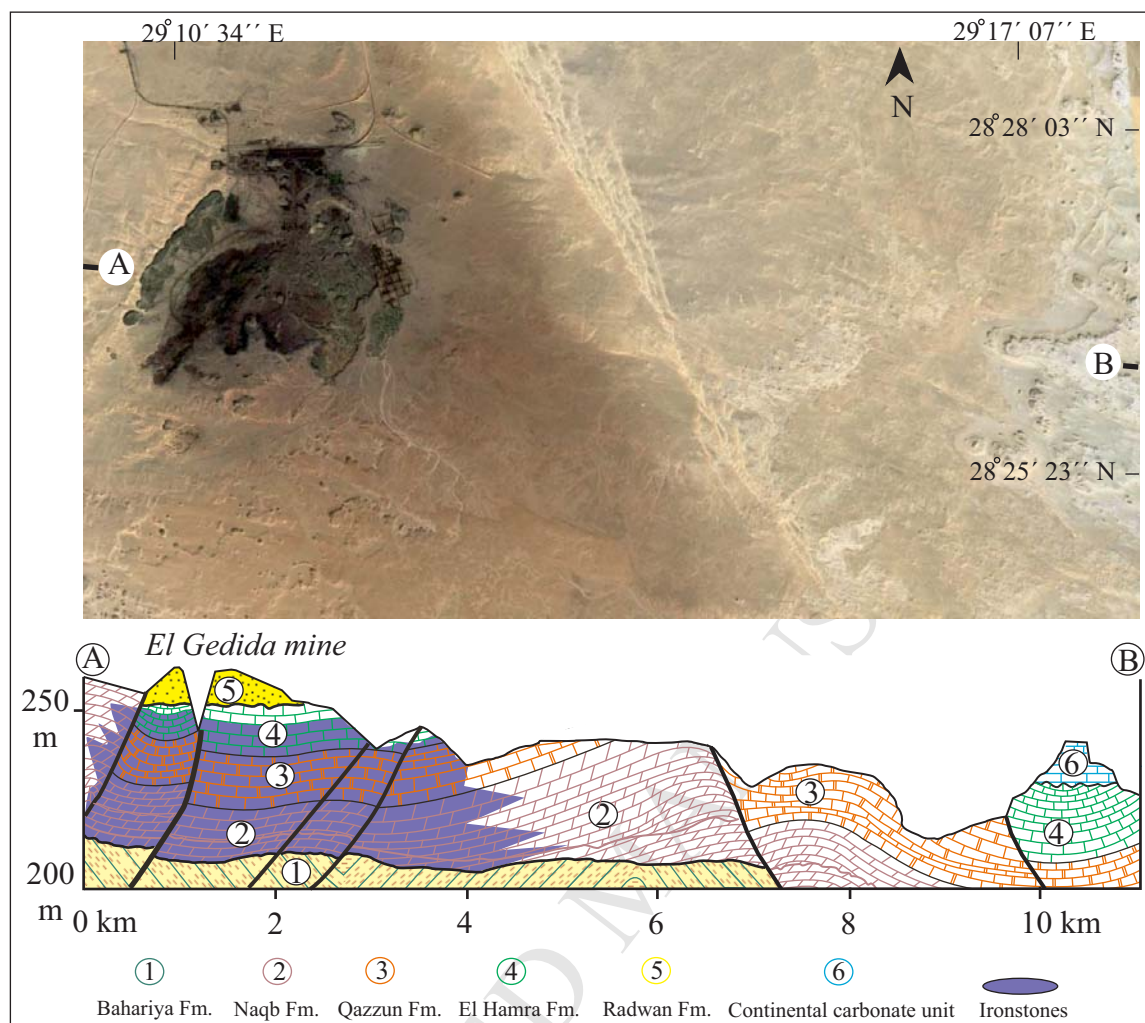


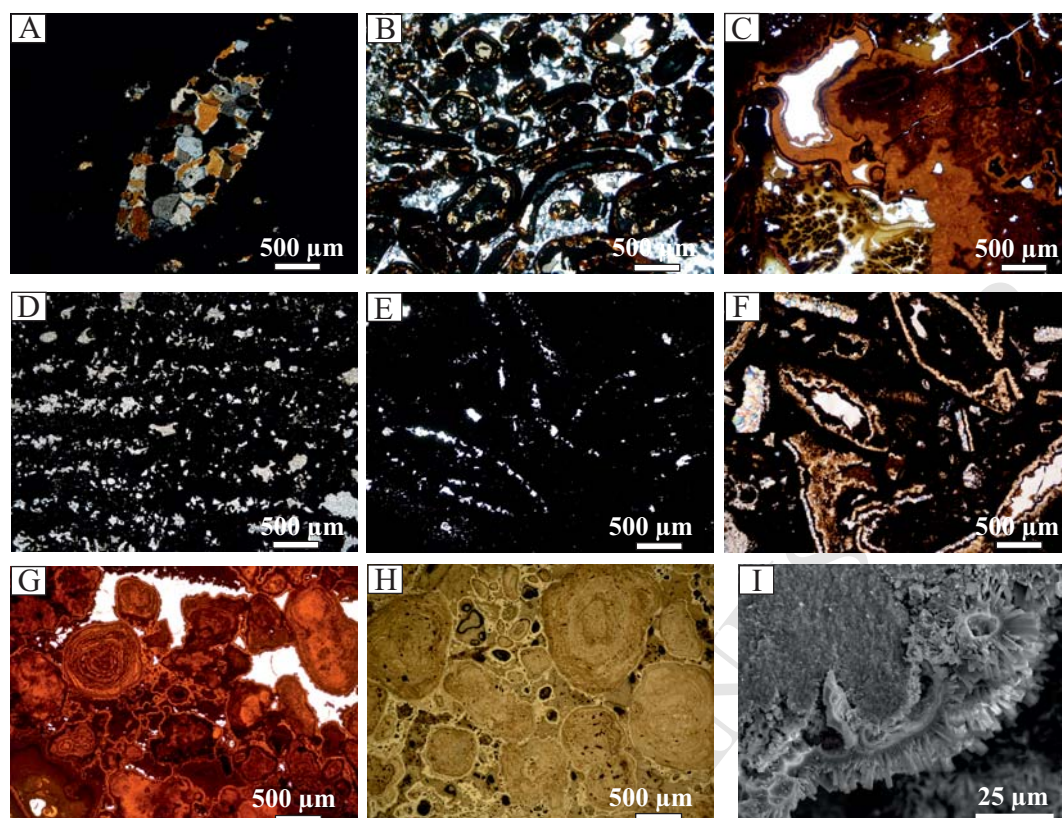


ACCEPTED MANUSCRIPT




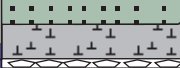




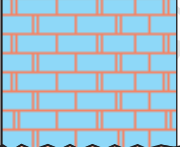








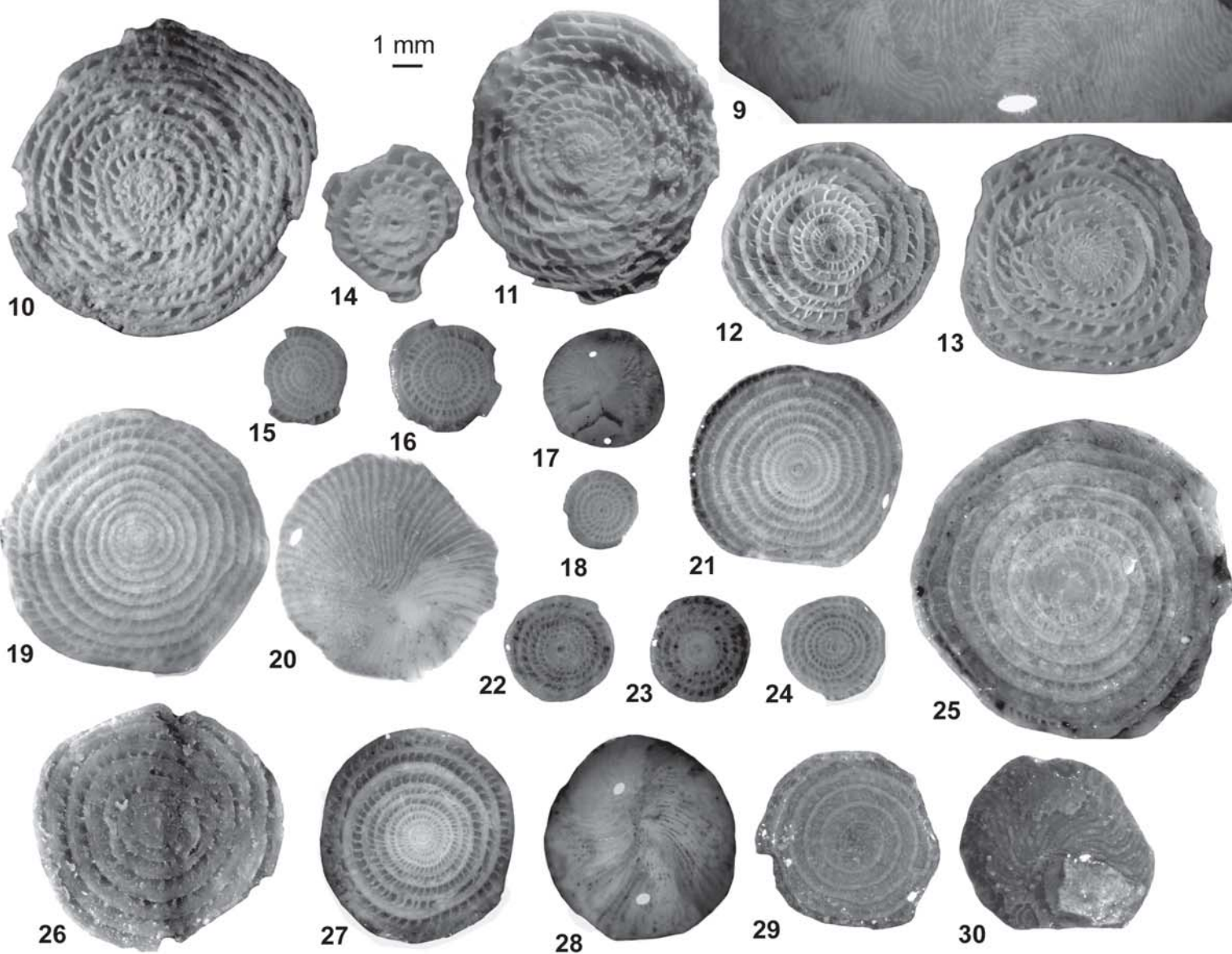
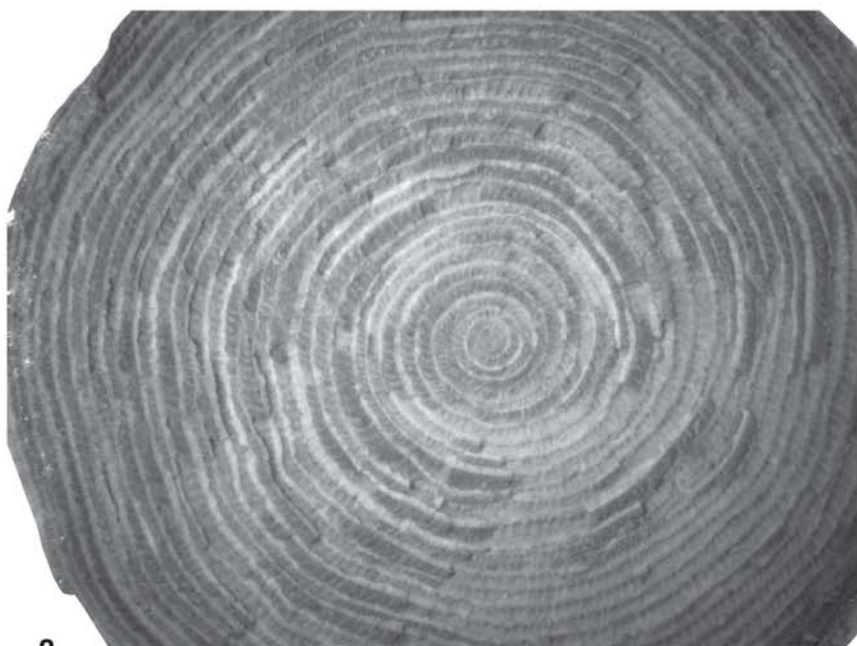
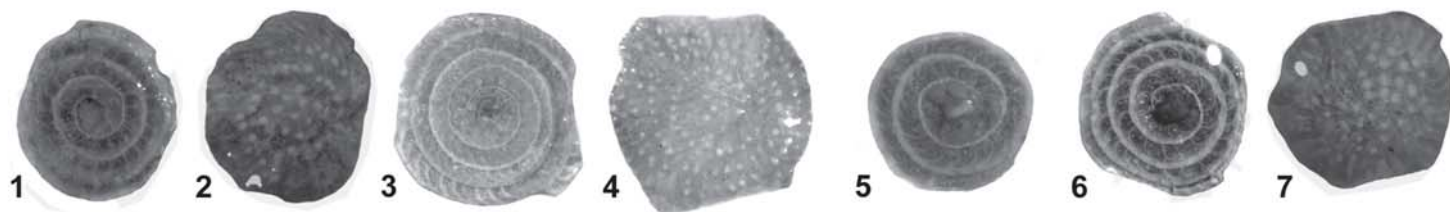






<i>Nummulites</i> Species			SBZ	Time Unit		Rock Unit	
				Priabonian		Upper Hamra	El Hamra Formation
				late	Bartonian		
<i>N. biarritzensis</i>	<i>N. lyelli</i>		SBZ 17	early		Lutetian	
<i>N. gizehensis</i> — <i>N. discorbinus</i>		<i>N. beaumonti</i>	SBZ 16	late			
			SBZ 15	middle			
			SBZ 14				
<i>N. praelorioli</i>		<i>N. migiurtinus</i>	SBZ 13	early	Qazzun Formation		
		<i>N. syrticus</i>	SBZ 12	late			
					late	Ypresian	

Age	Rock unit		SBZ	Section	Main lithologies
Oligocene	Radwan Formation				Sandstone
Bartonian/ Priabonian	El Hamra Formation (60 m)	Upper Hamra	SBZ19/ SBZ18	  	Fossiliferous siltstone Fossiliferous glauconitic packstone Fossiliferous siltstone
		Lower Hamra	SBZ17/ SBZ15	  	Fossiliferous wackestone/ packstone Nummulitic wackestone/ packstone Oyster rudstone
			SBZ14/ SBZ13		Fossiliferous wackestone/ packstone
		Qazzun Formation (30 m)	SBZ 13		Nummulitic wackestone/ packstone
Ypresian	middle-late Ilerdian (13 m)	Upper Sequence	SBZ9/ SBZ6	  	Bivalve dolostone Stromatolite-like laminated dolostone Fine laminated non-fossiliferous dolostone
		Lower Sequence		  	Brecciated non-fossiliferous dolostone Oolitic and fossiliferous dolostone Nummulitic dolostone
Cenomanian	Bahariya Formation				Siliciclastic rocks



## Highlights

- The chronostratigraphic framework of Eocene succession in Central Egypt is updated.
- The carbonate succession represents a long record of Eocene strata.
- Eight *Nummulites* species spanning the late Ypresian-early Bartonian are identified.
- Ironstone formation took place later than the early Bartonian, mostly in the Priabonian.
- Age dating of iron mineralization is crucial to explain its genesis.